



## Predictive models for multibiometric systems



Suresh Kumar Ramachandran Nair<sup>a</sup>, Bir Bhanu<sup>a</sup>, Subir Ghosh<sup>b</sup>, Ninad S. Thakoor<sup>a,\*</sup>

<sup>a</sup> Center for Research in Intelligent Systems, University of California, Riverside, CA 92521, USA

<sup>b</sup> Department of Statistics, University of California, Riverside, CA 92521, USA

### ARTICLE INFO

#### Article history:

Received 15 May 2013

Received in revised form

2 May 2014

Accepted 29 May 2014

Available online 9 June 2014

#### Keywords:

Object recognition

Biometrics

Modeling and prediction

Statistical models

### ABSTRACT

Recognizing a subject given a set of biometrics is a fundamental pattern recognition problem. This paper builds novel statistical models for multibiometric systems using geometric and multinomial distributions. These models are generic as they are only based on the similarity scores produced by a recognition system. They predict the bounds on the range of indices within which a test subject is likely to be present in a sorted set of similarity scores. These bounds are then used in the multibiometric recognition system to predict a smaller subset of subjects from the database as probable candidates for a given test subject. Experimental results show that the proposed models enhance the recognition rate beyond the underlying matching algorithms for multiple face views, fingerprints, palm prints, irises and their combinations.

© 2014 Elsevier Ltd. All rights reserved.

### 1. Introduction

Biometric systems are increasingly being deployed for identification, access control and surveillance [1]. Traditional deployments were mainly unimodal biometric systems which used a single sample from a single biometric modality. Performance of such systems suffered from noisy data, intra-class variations, inter-class similarities, non-universality and spoofing [2]. Some of these problems are addressed by using multibiometrics [2,3].

The term multibiometrics is used to denote three distinct classes of biometric systems: *multisample*, *multiview* and *multimodal*. In multisample biometrics, multiple samples are obtained from the same modality without any change in parameters. Examples are multiple images of the frontal view of the face, fingerprints of the same finger, iris images of the same eye etc. It has been shown that multisample biometrics can provide better recognition results compared to single sample results [4,5].

In multiview biometrics, samples are taken from the same biometric modality but under different conditions such as different face poses, different fingers, and different irises. Face recognition using multiple poses of face images, person identification using ten-print fingerprints, video based face recognition of walking persons etc. constitute examples of multiview biometric systems.

In multimodal biometrics, samples from different biometric modalities such as face, fingerprint, palmprint, iris, etc. are used. Multimodal biometrics provide better and robust authentication

and security [3] compared to unimodal biometric systems. A very visible use of multimodal biometrics is the US-VISIT program where the ten fingerprints, face and iris images of all international visitors are collected [6].

Even with multibiometrics, the matching subject returned by the recognition system may not be the true match [7]. Thus, a biometric recognition system generally provides a set of ranked matching subjects instead of just one matching subject. The performance of a biometric recognition system is typically characterized by the Cumulative Match Characteristic (CMC) Curve which provides a plot of the identification rate against rank  $k$ , where  $k$  is the number of top candidates [7].

This paper describes novel and generic statistical predictive models, which can predict the matching subjects in a multiview/multimodal biometric environment, depending on whether the *view details* of the test subject are known or not. By *view details* we mean the specific face pose (frontal, profile, etc.), the specific finger from which the fingerprint is taken, etc. The first model is called the Multinomial Model (MM) and is based on multinomial probability distribution. The second is called the Geometric Model (GM) and is based on geometric probability distribution. Both the approaches model the similarity scores produced when a test subject is matched against all the subjects in a database, and therefore, they are generic in nature. They can be applied to any biometric, provided a matching algorithm for that biometric is available. The models proposed in the paper model the score distributions and draw inferences regarding retrieval rankings based on those models. They do not explicitly model the recognition systems. The term predictive is used to emphasize the application of the models as the models are used to predict the ranking of the retrievals.

\* Corresponding author. Tel.: +1 951 827 3954.

E-mail addresses: [suresh.kumar@email.ucr.edu](mailto:suresh.kumar@email.ucr.edu) (S.K.R. Nair), [bhanu@cris.ucr.edu](mailto:bhanu@cris.ucr.edu) (B. Bhanu), [subir.ghosh@ucr.edu](mailto:subir.ghosh@ucr.edu) (S. Ghosh), [ninadt@ucr.edu](mailto:ninadt@ucr.edu) (N.S. Thakoor).

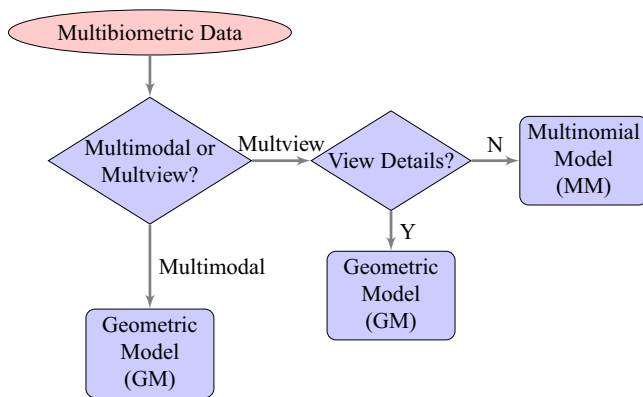


Fig. 1. Which model (GM or MM) to use for prediction?

The GM can be used in multiview systems where the view details are known. GM can also be used for predicting the matching subjects in multimodal biometric systems as the modality information of the test subjects is obviously available (e.g., it will be known if the test image is a fingerprint, palm print, etc.). The MM is suited for the multiview situations where the view details of the test subject are not known in advance. This can occur, for example, in surveillance systems where multiple views of a non-cooperative subject are matched against all the views present in a database. The flow chart in Fig. 1 shows how to choose the appropriate model based on the problem. Our prediction models are validated on a variety of publicly available databases of fingerprints, faces, palms, and irises.

When data from different biometric samples or modalities are available, an overall recognition result is typically obtained by fusing the individual results [4]. Therefore, the experimental results in this paper are compared with fusion results.

The paper is organized as follows. Section 2 describes the related work and our contributions. Section 3 describes the technical approach which begins with an overview and is followed by the detailed descriptions of both the proposed statistical models. Section 4 describes the results of our experiments on five different databases and Section 5 concludes the paper.

## 2. Related works and contributions

### 2.1. Related work

Typically, the different aspects of performance of a recognition system are predicted by modeling either the similarity scores or the feature space. A summary of the representative research in these areas is provided in this subsection.

Many researchers have used binomial probability distributions for modeling the similarity scores. Wayman [8] used them under the assumption of independence of errors, to estimate the probability that a false match never occurs. The paper derived equations for error rate. Daugman [9] described the use of binomial models for predicting whether the given distance metric belongs to the same iris or different irises. This is achieved by noting that the distance metric for similar and dissimilar pair of irises falls into two distinct binomial distributions. However it has been reported in [10] that the models proposed by [8,9] predicted exponential decrease in recognition rate when the database size increased while in reality the decrease is linear in the logarithm of the database size.

The face recognition vendor test report 2002 [10] provided another model for predicting the identification rate using the moments of the match score distribution. But the model underestimated the

identification rates. The model was based on the assumption that the similarity scores are independent and identically distributed. In practice this assumption needs not to be valid. Jhonson et al. [11] presented a method to estimate recognition performance for large galleries of individuals using data from a significantly smaller gallery. This was achieved by modeling the CMC curve using binomial distribution. The same problem has been addressed in a different way by Wang and Bhanu [12] for fingerprint recognition with the additional assumption that the match and nonmatch score distributions remain the same when the gallery size is increased. Grother and Phillips [13] presented the prediction of the recognition performance of large sized biometric galleries using a binomial model under the assumption that the match score distribution and the nonmatch score distribution are independent. Dass et al. [14] predicted confidence regions based on the Receiver Operating Characteristic (ROC) curve. This was accomplished by estimating genuine and imposter distributions of similarity scores through Gaussian copula models.

In contrast to the above, Wang et al. [15] presented an approach where performance prediction was used to increase the recognition rate which is the theme of this paper as well. Even though their method is generic, the increase in the recognition rate is achieved by discarding poor quality test subjects from the testing process. The poor quality test subjects are identified using a SVM classifier. In comparison, the work presented in this paper, builds statistical models for predicting matching subjects and achieves a higher recognition rate compared to the underlying matching algorithm by using all test subjects.

The research related to performance prediction where the feature space is modeled is described below. Schmid and O'Sullivan [16] described a framework for determining the performance of physical signature authentication based on likelihood models. Vectors of features extracted from the signatures were modeled as realizations of random processes. These random processes and the resulting distributions on the measurements determined bounds on the performance, regardless of the implementation of the recognition system. Boshra and Bhanu [17] presented a different approach to predicting probability of correct recognition by modeling the uncertainty, clutter, and occlusion of the 2D feature vectors of a subject which was verified on synthetic aperture radar data. In [18], Aggrawal et al. proposed a framework for predicting the success and failure of an algorithm in a face verification scenario. This method is specific to face recognition. Pankanti et al. [19] studied individuality of fingerprints, meaning they estimated the probability that two fingerprints from two different fingers are considered to be the same. Tan and Bhanu [20] provided an improvement over [19] with a two-point model and a three-point model to estimate the error rate for the minutiae based fingerprint recognition. The approach measured minutiae's position and orientation, and the relations between different minutiae to find the probability of correspondence between fingerprints. They allowed overlap of the uncertainty area of any two minutiae.

### 2.2. Contributions

1. The paper develops novel and generic statistical models, which are independent of the biometrics and the matching algorithm, for predicting the matching subjects in a multi-biometric recognition system. In our preliminary work [21], we used the geometric model for predicting indexing performance.
2. The paper shows that using the proposed framework enhances the recognition rate of the underlying matching algorithm for different biometrics.
3. The proposed prediction model is validated on several publicly available databases of face, fingerprint, iris, and palmprint.

### 3. Technical approach

#### 3.1. Overview

Given a multibiometric recognition system, the objective is to predict the possible matching subjects corresponding to a given test subject, from a database of subjects. This subsection describes the organization of the database, the process of generating the similarity scores, and the testing procedure for the proposed models. How the models are trained is described in detail in Sections 3.2 and 3.3.

Consider the case where a multinomial model (MM) is used (see Fig. 1). A single database is used to store subjects corresponding to  $V$  views of each of the subjects. If the database contains subjects corresponding to  $G$  different subjects, it will have  $G \times V$  subjects in it. All views of the same subject are stored in consecutive positions in the database. Fig. 2 shows the organization of the database for  $V=3$ . It contains frontal, half left and half right face images of three subjects. When a subject is to be identified from this database,

$V$  views of a test subject are given and all of them are matched against  $G \times V$  subjects present in the database generating  $G \times V \times V$  similarity scores. It may be noted that at the time of testing, the specific view to which the given test subject belongs to, need not be known. Note that in the set of  $G \times V^2$  similarity scores,  $V$  of them are match scores and the remaining are nonmatch scores.

As seen from Fig. 1, the geometric model (GM) is used in two different situations and, therefore,  $V$  may represent either the number of views or the number of different modalities used. In both cases,  $V$  different databases of subjects are maintained. Each database contains the subjects corresponding to a specific modality or a specific view. The subjects are kept in the same order as the subjects in all the  $V$  databases. When a subject is to be identified,  $V$  views of the subject are available and each of them are matched against all the subjects in the corresponding database only and the process generates  $G \times V$  similarity scores per database. Fig. 3 shows the organization of the database for  $V=3$ . There are three different databases where each one contains the face, palm print and iris images of three subjects.

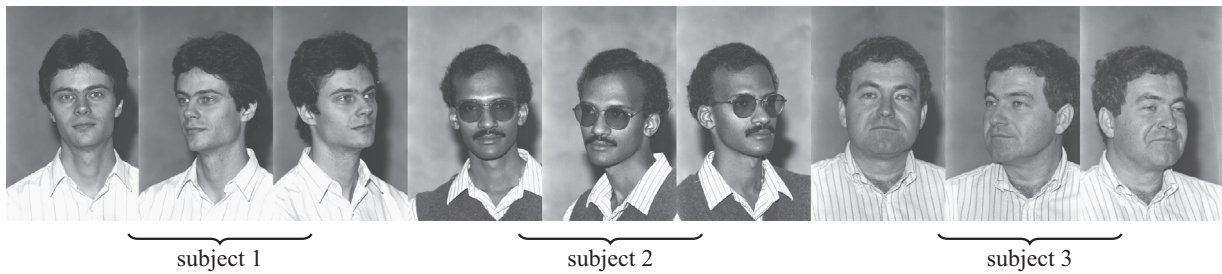


Fig. 2. Organization of database for multiview systems,  $G=3, V=3$ .

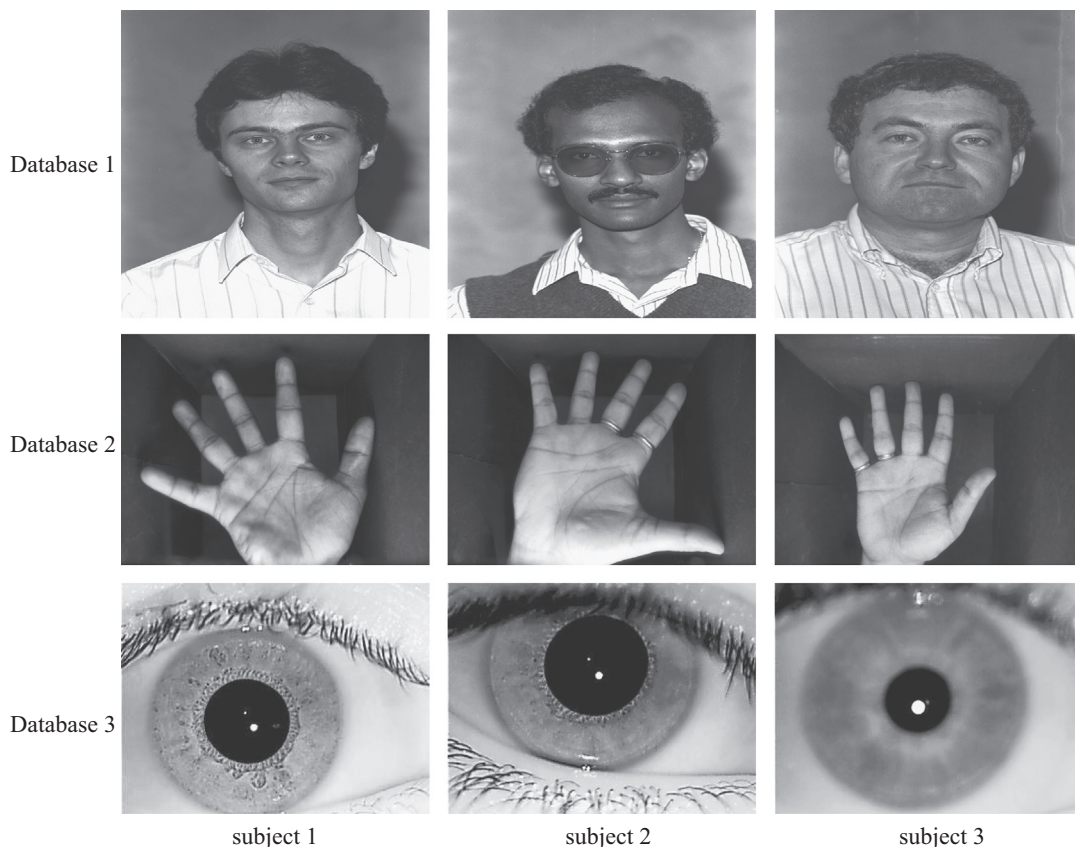
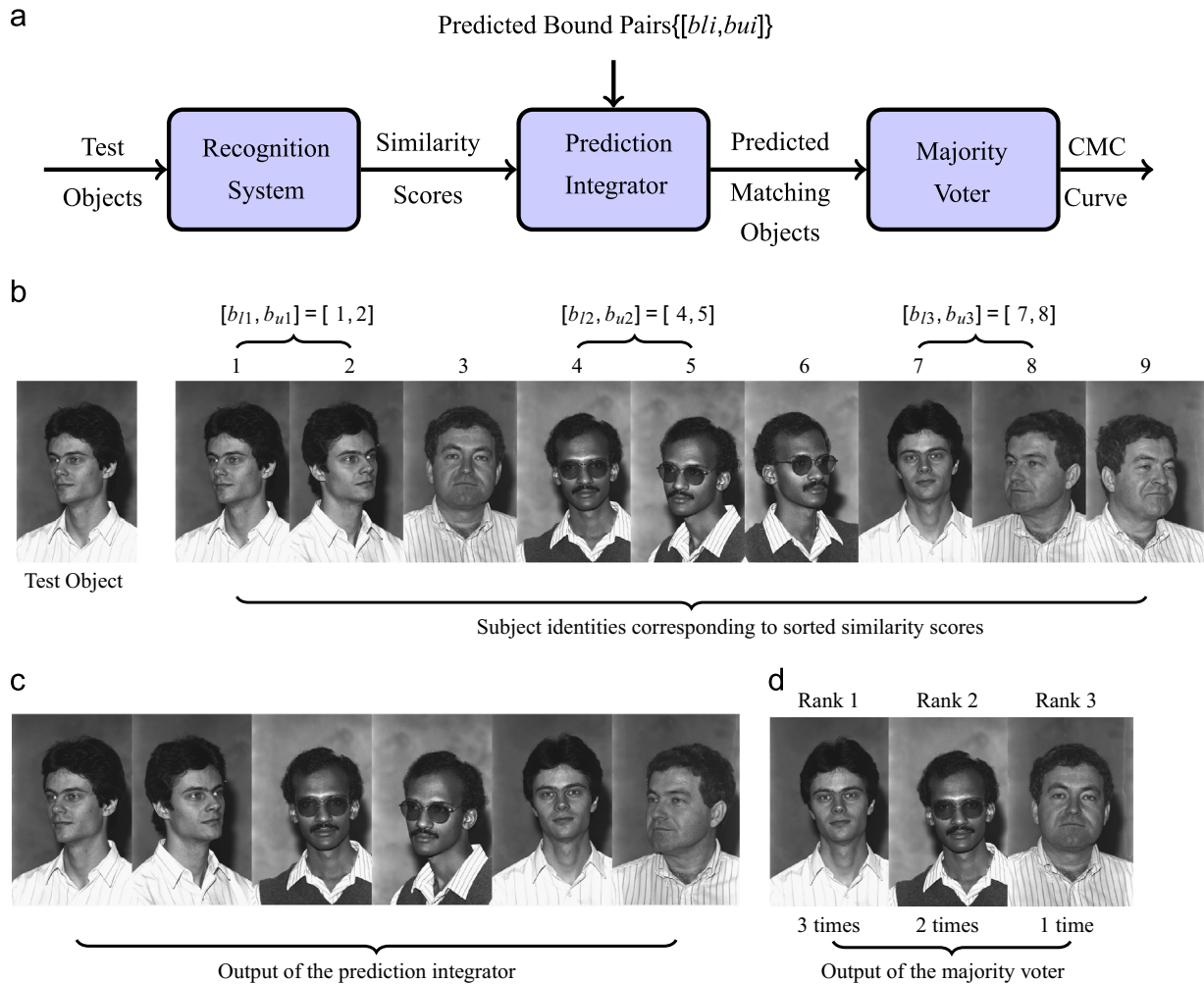


Fig. 3. Organization of database for multimodal systems,  $G=3, V=3$ . There are three different databases where each one contains a particular modality from all subjects.



**Fig. 4.** (a) The block diagram representation of the validation process. Note that in the case of geometric model the value of  $b_{li}$  is always 1. (b)–(d) Illustration of the validation process for multinomial model for  $G=3$ ,  $V=3$ . The bounds predicted by the model were  $\{\{1, 2\}, \{4, 5\}, \{7, 8\}\}$ . (b) Subject ids corresponding to the sorted similarity scores from the recognition system. (c) Output of the prediction integrator obtained by examining the bounds  $\{\{1, 2\}, \{4, 5\}, \{7, 8\}\}$  in  $S_s$  from (b). (d) Output of the majority voter sorted in the increasing order of ranks which is same as the decreasing order of frequencies. In this figure, the subject ids are represented by their frontal faces for easiness of illustration.

After training (details described in Sections 3.2 and 3.3), the multinomial and geometric models generate  $V$  pairs of index bounds. In the case of the multinomial model, the index bounds are of the form  $\{\{b_{l1}, b_{u1}\}, \dots, \{b_{lV}, b_{uV}\}\}$ . When the geometric model is used, there are  $V$  different databases and each database produces an index bound of the form  $[1, b_{ui}]$  where  $1 \leq i \leq V$ . Note that the lower bound of the index is always 1 in the case of the geometric model. As could be expected, the index bounds do not change once the training is over.

The validation process in the case of multinomial model is described below. As mentioned earlier in this section,  $G \times V \times V$  similarity scores are produced by  $V$  views of a test subject. These similarity scores are sorted in the ascending order. In this paper, we assume that lower the similarity score, the better the match is. The models presented in the paper are applicable in the opposite case also by appropriately modifying the similarity score values. We assume that an instance of the test subject is present in the database (closed recognition system [13]). The sorted similarity scores and the index bounds  $\{\{b_{l1}, b_{u1}\}, \dots, \{b_{lV}, b_{uV}\}\}$  predicted by the multinomial model are given to the prediction integrator as shown in Fig. 4(a).

The prediction integrator examines the subject identities (ids) of the similarity scores falling in the intervals  $\{\{b_{l1}, b_{u1}\}, \dots, \{b_{lV}, b_{uV}\}\}$ . As the database has  $V$  views of the same subject, the prediction

integrator output may contain the same subject identity (id) multiple times. The output of the prediction integrator is given to the majority voter as shown in Fig. 4(a). The majority voter sorts the subject ids in the descending order of frequency of occurrence. Thus, the output of the majority voter represents the predicted matching subjects in the decreasing order of ranks. The first subject id in this list is the rank 1 output of the prediction system, the second one in the list is the rank 2 output, and so on. This process is illustrated in Fig. 4. With a set of test subjects, by noting the rank of the matching subject id in the output of the majority voter, a CMC curve is plotted. If the corresponding subject id is not present in the output, the prediction is deemed a failure.

In the case of geometric model, there are  $V$  databases and  $V$  predicted bounds for each database in the form  $[1, b_{ui}]$ ,  $1 \leq i \leq V$ . When  $V$  test subjects are given, each one is compared against all subjects present in the *corresponding* database and a set of  $G$  sorted similarity scores are produced. Note that in each of these  $G$  scores only one score is the match score and the remaining are the nonmatch scores. The prediction integrator receives the sorted similarity scores from all the  $V$  databases and the  $V$  predicted bounds  $\{\{1, b_{u1}\}, \dots, \{1, b_{uV}\}\}$ . From now on, the process is exactly similar to that for the MM system. A comparison of both models is given in Table 1.

**Table 1**  
Comparison of Geometric and Multinomial models.

Geometric model	Multinomial model
1 $V$ different databases (see Fig. 3)	One database (see Fig. 2)
2 $V$ views or modalities per subject for training	$V$ views per subject for training
3 $V$ or less than $V$ biometrics per subject are required for testing	Exactly $V$ biometrics per subject are required for testing
4 Each database contains subjects corresponding to the same view or modality	All views of the same subject are stored in subsequent positions in the database
5 $V$ test subjects produces $G$ similarity scores per database and altogether $GV$ similarity scores from all databases	$V$ test subjects produces $GV^2$ similarity scores
6 One bound predicted per database and thus a total of $V$ bounds predicted	$V$ bounds are predicted
7 The bounds are of the form $[1, b_{ui}], 1 \leq i \leq V$	The bounds are of the form $[b_{li}, b_{ui}], 1 \leq i \leq V$
8 The view/modality of subjects must be known at the time of testing	The view information of test subjects is not required
9 $V$ different recognition systems may be used if multimodal data is used	Only one recognition system is used

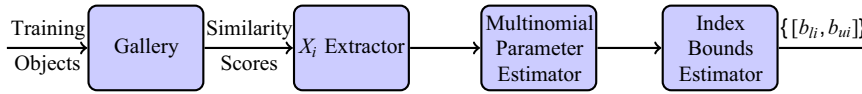


Fig. 5. Training the multinomial model.

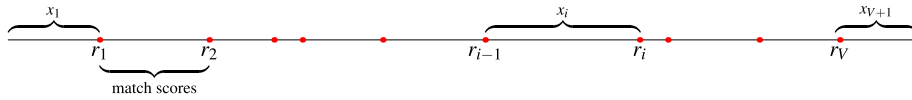


Fig. 6. Ordering of match and non-matched scores in  $S_s$ .

Since the GM based approach is modular, it is not necessary that  $V$  views or modalities of the test subject be available for identifying the subject. The process described in the paper would work without any modification, even if only less than  $V$  views and modalities are known at the time of testing.

3.2. Training the multinomial model

Fig. 5 shows steps in training the Multinomial model. The purpose of the model is to predict the index bounds within which the matching subject is likely to be present, in a sorted set of similarity scores  $S_s$ . For accomplishing this, we will model the index of the match score ( $r_i$ ) or equivalently the count of the nonmatch scores present between the match scores ( $x_i$ ). The  $r_i$  and  $x_i$  are pictorially shown in Fig. 6. Let us assume that  $r_i$ s are instances of a random variable  $R_i$ . Let us identify the properties of  $R_i$  in order to model them. First we note that, it takes integer values ranging from 1 to  $NV$ . Here  $N$  is the total size of the database ( $N=GV$  for multinomial and  $N=G$  for geometric models). If we assume that the recognition system being modeled behaves closer to an ideal system, the values of  $r_i$  would still range from 1 to a number greater than or equal to  $V$ . Nothing more can be said about the properties of  $R_i$  and hence it is difficult to model them. However if we assume  $x_i$  to be an instance of the random variable  $X_i$  it has an important property that its value is always small (zero for an ideal system) except for  $x_{V+1}$ . The properties of the random variable  $X_i$  are given below. Let  $x_i$  be observed instances of  $X_i$  and  $\mathbb{Z}$  be the set of integers.

**Property 1.**  $x_i \in \mathbb{Z}$ .

**Property 2.** In a recognition system, the value of  $x_i$  would be small compared to  $V(N-1)$ , the total number of non-match scores except in the case of  $x_{V+1}$ .

**Property 3.**  $\sum_{i=1}^{V+1} x_i = V(N-1)$ .

Properties 1 and 2 suggest that  $x_i$  is a small integer valued random variable which could be modeled using the Poisson

distribution. The Poisson random variable is typically used to model the number of misprints in a book or the number of accidents taking place at a particular location in a given time, etc. [22]. Our situation is similar in the sense that the values of  $x_i$  would be very small, zero ideally, compared to the maximum possible value of  $V(N-1)$  except in the case of  $x_{V+1}$ . The suitability of Poisson distribution can also be justified by visually comparing the Poisson distribution and the distribution of  $X_i$  obtained in our experiments as shown in Fig. 7. Note that there are other distributions which fit these properties as well, however we choose the Poisson random variable due to its simplicity. Next we describe, how the joint distributions of  $X_i$  could be obtained.

3.2.1. Modeling the joint distribution of  $X_i$

As described in the previous section, we assume that  $X_i$ 's are independent of the Poisson random variables.  $X_i$ 's have an interesting property that their sum is a constant (Property 3). Using this, it can be shown that the joint distribution of  $X_1, \dots, X_{V+1}$  is multinomial [24].

$$f\left(X_1 = k_1, \dots, X_{V+1} = k_{V+1} \mid \left(\sum_{i=1}^{V+1} X_i = V(N-1)\right)\right) = \frac{(V(N-1))!}{k_1! \dots k_{V+1}!} p_1^{k_1} \dots p_{V+1}^{k_{V+1}} \quad (1)$$

where

$$p_i = \frac{\lambda_i}{\lambda_1 + \dots + \lambda_{V+1}}, \quad 1 \leq i \leq V+1 \quad (2)$$

This is an important property which enables us to use the Poisson/Multinomial distribution for our problem. The multinomial distribution is a generalization of binomial distribution. It is used in chemical engineering applications where the possible outcome could be in more than two categories (temperature={high, med, low}). Multinomial systems are a useful analysis tool when a “success–failure” description is insufficient to understand a chemical engineering system [25]. The mixture of multinomial models is extensively used in text classification [26].

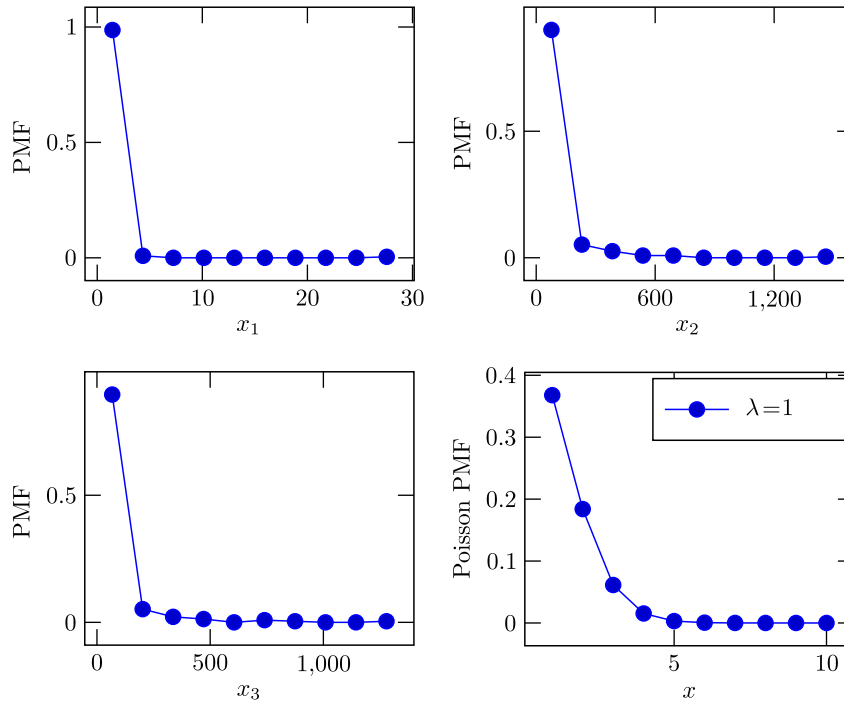


Fig. 7. Visual comparison of the probability mass function (PMF) of  $X_i$  with Poisson distribution. The PMF of  $x_1, \dots, x_3$ , generated from the color FERET database [23] and the PMF of Poisson distribution. Note the similarity of the PMFs of  $x_i$  with that of Poisson distribution. The horizontal axes have different scales as each distribution is characterized by a different value of the parameter  $\lambda$ .

With the sorted similarity scores being available, we first estimate the probability  $p_i$  that a given non-match score will fall between match scores with index  $r_i$  and  $r_{i-1}$ . This is done under the assumption of cumulative odds probability model [27]. We note that a non-match score can be above or below the  $i$ th match score,  $i = 1, \dots, V$ . The cumulative odds for a non-match score relative to the  $i$ th match score,  $\theta_i, i = 1, \dots, V$ , are

$$\theta_i = \frac{p_1 + p_2 + \dots + p_i}{p_{i+1} + p_{i+2} + \dots + p_{V+1}} \quad (3)$$

We define

$$\log \theta_i = \beta_i \quad (4)$$

From (3), we get

$$\log \theta_1 = \log \frac{p_1}{p_2 + \dots + p_{V+1}} = \log \frac{p_1}{1 - p_1} = \beta_1 \quad (5)$$

$$\text{Hence } p_1 = \frac{e^{\beta_1}}{1 + e^{\beta_1}} = \frac{\theta_1}{1 + \theta_1} \quad (6)$$

Similarly, from (3) we have

$$\log \theta_2 = \log \frac{p_1 + p_2}{1 - p_1 - p_2} = \beta_2 \quad (7)$$

Thus,

$$p_1 + p_2 = \frac{e^{\beta_2}}{1 + e^{\beta_2}} = \frac{\theta_2}{1 + \theta_2} \quad (8)$$

Extending the above, we get

$$p_1 + \dots + p_V = \frac{\theta_V}{1 + \theta_V} \quad (9)$$

$$p_{V+1} = \frac{1}{1 + \theta_V} \quad (10)$$

### 3.2.2. Estimation of the multinomial cumulative odds model parameters

We want to estimate the parameters  $\theta_1, \dots, \theta_V$ . From (6), (9), and (10)

$$p_i = \frac{\theta_i}{1 + \theta_i} - \frac{\theta_{i-1}}{1 + \theta_{i-1}}, \quad i = 2, \dots, V \quad (11)$$

From Eq. (1), the likelihood function, ignoring terms that do not involve  $\theta_i$  is

$$L = \left(\frac{\theta_1}{1 + \theta_1}\right)^{x_1} \left(\frac{\theta_2 - \theta_1}{(1 + \theta_1)(1 + \theta_2)}\right)^{x_2} \dots \left(\frac{\theta_V - \theta_{V-1}}{(1 + \theta_V)(1 + \theta_{V-1})}\right)^{x_V} \left(\frac{1}{1 + \theta_V}\right)^{x_{V+1}} \quad (12)$$

Differentiating the logarithm of the likelihood function w.r.t.  $\theta_i$  and equating to zero we find

$$\frac{x_1}{\hat{\theta}_1} - \frac{x_2}{\hat{\theta}_2 - \hat{\theta}_1} - \frac{x_1 + x_2}{1 + \hat{\theta}_1} = 0 \quad (13)$$

$$\frac{x_2}{\hat{\theta}_2 - \hat{\theta}_1} - \frac{x_3}{\hat{\theta}_3 - \hat{\theta}_2} - \frac{x_2 + x_3}{1 + \hat{\theta}_2} = 0 \quad (14)$$

⋮

$$\frac{x_V}{\hat{\theta}_V - \hat{\theta}_{V-1}} - \frac{x_V + x_{V+1}}{1 + \hat{\theta}_V} = 0 \quad (15)$$

Solving equations from (13)–(15) we get the maximum likelihood estimate of  $\theta_i$  as

$$\hat{\theta}_i = \frac{\sum_{k=1}^i x_k}{\sum_{k=i+1}^{V+1} x_k} \quad (16)$$

Substituting for  $\theta_i$  in (6), (10), (11) we get the estimates of probabilities.

### 3.2.3. Predicting the index of the $i$ th match score

The probability that  $r_i$  is the index of the  $i$ th match score is the same as the probability that  $\sum_{k=1}^{r_i-i} x_k = r_i - i$  non-match scores are present before  $r_i$ . The probability that a non-match score will be before  $r_i$  is  $p = \sum_{k=1}^{r_i-i} p_k$ . Thus, the required probability can be expressed as a binomial probability

$$P_{r_i-i} = \binom{V(N-1)}{r_i-i} p^{r_i-i} (1-p)^{V(N-1)-(r_i-i)} \quad (17)$$

### 3.2.4. Estimating the bounds of the indices

The 95% confidence interval, the bounds  $[b_l, b_u]$ , for  $r_i$  can be obtained by solving for  $b_l$  and  $b_u$  in the following equations [22]:

$$\sum_{k=0}^{b_l} \binom{n}{k} p^k (1-p)^{n-k} \approx 1 - F(p; b_l, n - b_l - 1) = 0.025 \quad (18)$$

$$\sum_{k=b_u}^n \binom{n}{k} p^k (1-p)^{n-k} \approx F(p; b_u - 1, n - b_u) = 0.025 \quad (19)$$

where  $F(x; \alpha, \beta)$  is the cumulative distribution of the incomplete beta function

$$F(x; \alpha, \beta) = \frac{(\alpha + \beta + 1)!}{\alpha! \beta!} \int_0^x t^\alpha (1-t)^\beta dt \quad (20)$$

The bounds for any other confidence level  $C$  may be calculated by replacing the right hand side of Eqs. (18) and (19) with  $(1-C)/200$ .

### 3.2.5. Robust estimation of the multinomial model parameters

During the training of the multinomial model, it was observed that a very small fraction of the  $X_i$  values were unusually large and from Eq. (16), it is clear that one such large value of  $X_i$  alone can push the estimated bounds farther from where it should be. The large values of  $X_i$  were the results of poor registration of images or because of the unusually high noise present in the data. Such large values of  $X_i$  are called outliers and outcomes of traditional statistical methods can possibly be distorted by such outliers [28]. In order to reduce the influence of outliers in the estimation of  $p_i$  (Eq. (2)), another estimation approach was used. Instead of estimating  $p_i$  using Eqs. (11) and (16), the Poisson parameter  $\lambda_i$  of  $X_i$ ,  $1 \leq i \leq V+1$  were estimated using robust estimation methods and they were substituted in Eq. (2). The robust estimation of the Poisson parameter was carried out using the `glmrob` function of the R statistical package [29]. It was found that the results obtained using robust estimation approaches were superior to that obtained from using maximum likelihood estimation, as outliers are common phenomena in real world scenarios.

## 3.3. Training the geometric model

Fig. 8 shows steps in training the geometric model. Unlike the multiview case where a single multinomial model and a single database are used,  $V$  different models and  $V$  different databases are used when the geometric model is used for prediction (see Table 1). If  $V$  different modalities are used, there could be  $V$  different recognition systems as well.

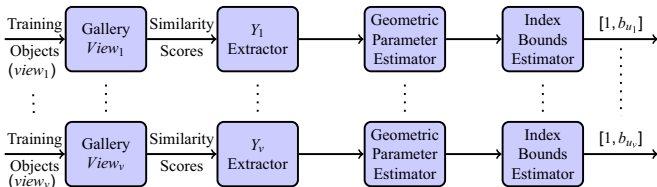


Fig. 8. Geometric model training.

Each database contains a specific view/modality of all the subjects. We are given  $V$  test subjects to identify a subject. Our objective is to find out how many top matches must be searched, in the ranked list of subjects returned by the recognition system to locate the correct matching subject for each of the  $V$  test subjects. Let  $k$  be the number of top ranking subjects that one should search to locate the matching subject. Then the bounds  $[b_l, b_u]$  take the form  $[1, k]$  as we are searching all the  $k$  top matches. As we have  $V$  databases, we need to predict  $V$  bounds of the form  $\{[1, b_{ui}], 1 \leq i \leq V\}$ .

As described in Section 3.2, this is best achieved by modeling the count of the nonmatch scores that appear before the match score, in the sorted list of similarity scores produced by the recognition system when a test subject (one among the  $V$  test subjects) is given, instead of directly modeling the position of the match score in  $S_s$ . Here also we assume a closed-set identification system [13].

Let  $Y$  be a random variable representing the count of the non-match scores present in a sorted set of similarity scores before the match score. If the recognition system is ideal, the value of  $Y$  would be zero. In order to build a statistical model, we present the properties of  $Y$

1.  $Y \in \mathbb{Z}$
2.  $Y \in [0, N - 1]$ .
3. Many times  $Y$  may have value equal to zero. Often, for a recognition system, the correct match score is the first one in the set of sorted similarity scores.

Considering the above properties one can see that  $Y$  can be modeled using geometric distribution [21]. Geometric distribution models the number of trials needed before the first success in repeated Bernoulli trials [30]. In our case, each element in the sorted set of similarity scores can be assumed to be coming from a Bernoulli trial (a given similarity score may be a match score or a non-match score) and if the score is a match score, we denote it as success and if the score is a non-match score, we denote it as failure. Thus, geometric distribution can model the number of non-match scores present before the match score. Besides, our requirement of high probability for very small values of  $Y$  is also satisfied by the geometric distribution. Note that while there are other distributions which might fit these properties as well, we choose Geometric distribution due to its simplicity.

The random variable  $Y$  is a waiting-time random variable (we wait till the match score is obtained) and the geometric distribution is a natural candidate model to describe the waiting-time random variable.

The suitability of geometric distribution can also be visually verified by observing the PMF of  $Y$  obtained from experiments and the PMF of a geometrically distributed random variable as shown in Fig. 9.

It may be noted that in the case of multiview systems (Section 3.2) the number of nonmatch scores was modeled as a Poisson random variable. Even though the random variables in both situations look similar, there are some key differences. In the multiview situation, we have  $V$  random variables whose sum has to be a constant. No such conditions exist in the present situation. Besides, the value of  $Y_i$  in the multiview case needs not to be zero for all  $i$  and at least  $Y_{V+1}$  would be a large in practice.

### 3.3.1. Estimation of geometric distribution parameter

Let  $Y$  be a geometrically distributed random variable. Then

$$P(Y = y) = p(1-p)^y \quad \text{where } y = 0, 1, \dots \quad (21)$$

Let  $y_1, y_2, \dots, y_T$  be the realizations of  $T$  independent and identically distributed geometrical trials described by the model in Eq. (21).

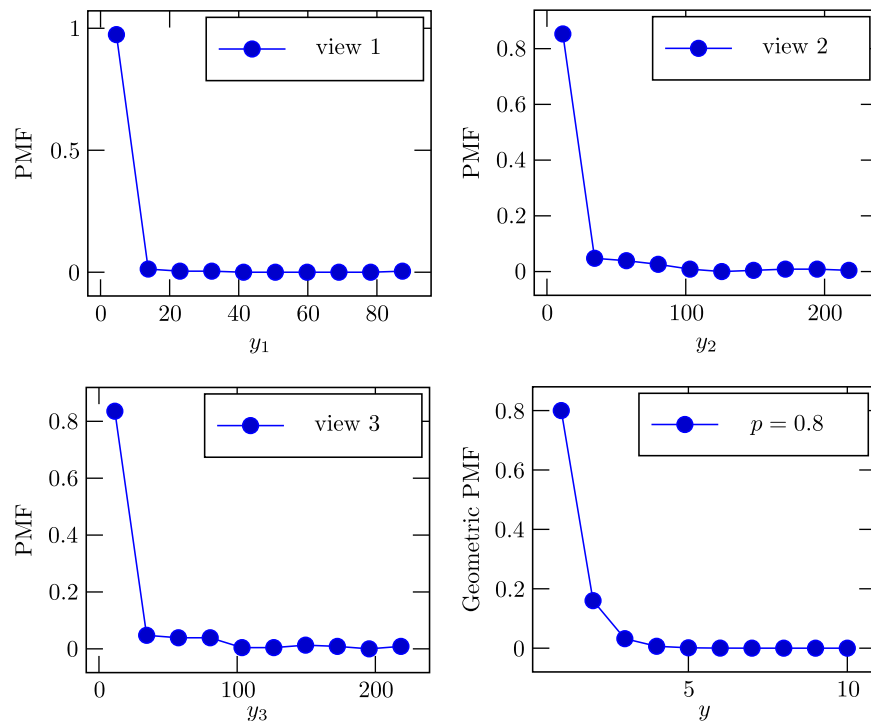


**Fig. 9.** PMF of  $Y$ , the number of non-match scores present before the match score. The first three figures show the PMF from the view 1, 2, 3 of the color FERET database. The last figure shows the PMF of geometric distribution obtained with  $p=0.8$ . Note the visual similarity between the PMFs. The horizontal axis has different scales as each distribution is characterized by a different value of the parameter  $p$ .

It can be shown that the value of  $p$  can be estimated using maximum likelihood approach.

$$\hat{p} = \left( 1 + \frac{1}{T} \sum_{i=1}^T y_i \right)^{-1} \quad (22)$$

### 3.3.2. Estimating the value of $k$ for a given confidence

The CDF of the geometric distribution is given by

$$F(y) = 1 - (1-p)^{y+1} \quad (23)$$

We need to find out the range of values of  $y$  which occur in 95% of the experimental trials. As  $Y$  is modeled as a geometric random variable, lower bound of  $y$  is obviously zero. The upper bound ( $b_u$ ) is given by the equation

$$F(b_u) = 1 - (1-p)^{b_u+1} = 0.95 \quad (24)$$

If there are  $b_u$  non-match scores before the first match score, then

$$k = b_u + 1 = \frac{\log 0.05}{\log(1-p)} \quad (25)$$

Thus the predicted bounds for a given confidence  $C$  would be

$$\left[ 1, \frac{\log(1-\frac{C}{100})}{\log(1-\hat{p})} \right] \quad (26)$$

## 4. Experimental results

We used the following five databases for our experiments: (1) Color FERET Database [23], (2) NIST-14 Ten-print Fingerprint Database [31], (3) The IIT Delhi Iris Database [32], (4) The IIT Delhi palmprint image database [33] and (5) NIST Biometric Scores Set – Release 1 (BSSR1) [34]. These datasets are chosen to demonstrate

the ability of our method to handle different types of biometrics. Additionally, as our goal is to show how the proposed theory can be applied independent of the underlying algorithms, in most cases we chose the scores provided by the dataset providers as our baseline. However, in some cases we find that these datasets have not been used under the same experimental conditions as ours. For these cases only it is not possible to provide a direct comparison with exiting work.

In [4,5], it was reported that the best multiview/multimodal results were obtained by fusing individual scores by adding them. Therefore, sum fusion results are used as the baseline for all of our experiments. As reported in [5], the scores were first normalized in the range [0, 100] and then added.

The experimental results are reported by plotting the CMC curves. Each figure contains the best and worst CMC curves of the individual view/modality, the results of multinomial model with and without robust estimation, geometric model and that of the sum fusion. Only the best/worst individual view/modality CMC curves are shown to avoid clutter in the figures.

In all the experiments the confidence is taken as 95% and 10-fold cross validation is used. A summary of the experiments conducted with various databases is shown in Table 2.

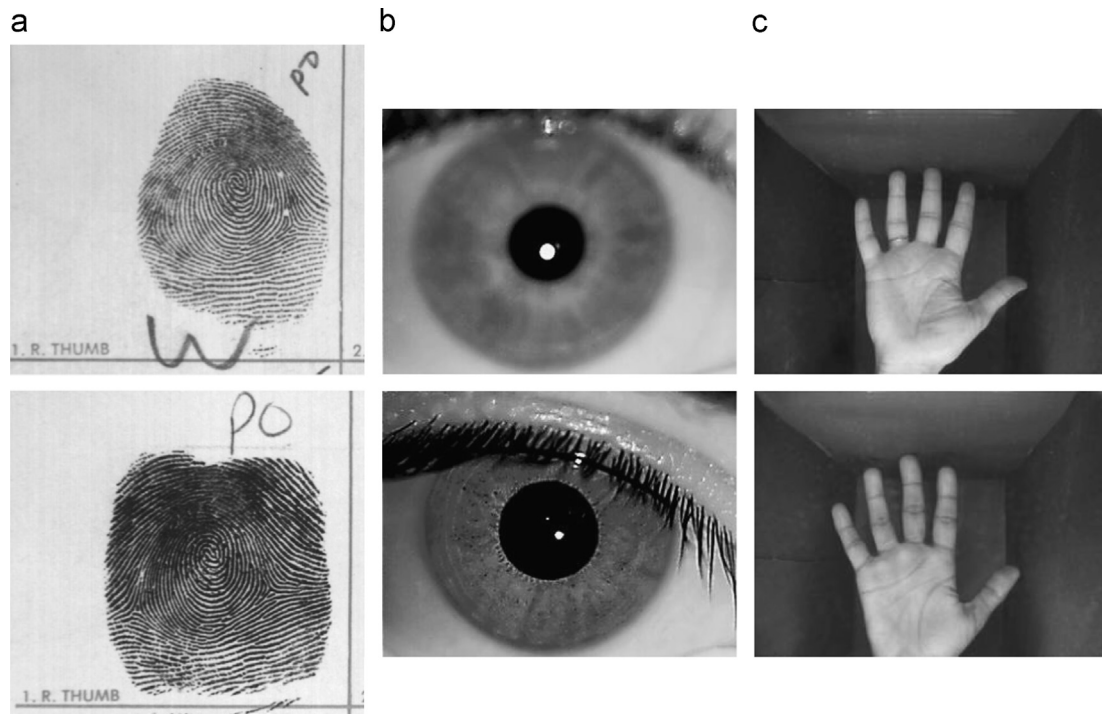
### 4.1. Results on color FERET database [23]

This database [23] contains a total of 11,338 facial images. They are collected by photographing 994 subjects at various angles, over the course of 15 sessions between 1993 and 1996. Sample images from this database are shown in Fig. 11. From this we select 231 subjects where each subject has five views available (frontal, half left, half right, profile left, and profile right) and at least two different instances of each of these views are available so that one instance can go into the database and the other instance can go into the test set. These images are first cropped to contain only the

**Table 2**

Summary of the experiments and the databases used.

No	Exp. type	Database	G	V	N	Results
1	Multiview	Color FERET	231	5	1155	Fig. 12
2		Color FERET without frontal face	231	4	924	Fig. 13
3		NIST-14 Fingerprints	2700	10	27,000	Fig. 14
4		IIT Delhi Iris	112	2	224	Fig. 15
5		IIT Delhi Palm	116	2	232	Fig. 16
6	Multi-modal/view	BSSR1 Left index finger, Face C	517	2		Fig. 17
7		BSSR1 Left index finger, Face G	517	2		
8		BSSR1 Right index finger, Face C	517	2		
9		BSSR1 Left index finger, Face G	517	2		
10		BSSR1 Left and Right Index Fingers	517	2		Fig. 18

**Fig. 10.** Sample images from (a) NIST-14 Database [31], (b) IIT Delhi Iris Database [32], and (c) IIT Delhi Touchless Palmprint Database [33].

face regions and then resized to  $200 \times 200$ . To align the facial features consistently for each view, each image is registered to a level 4 Avatar image [35]. The level 4 Avatar image for a view is computed from the database images for that view alone. After the registration, each image is split into 25 square blocks of size  $40 \times 40$ . Local Binary Pattern (LBP) histogram for each of the blocks is calculated and all 25 histograms are concatenated to form a single vector. LBPs are computed using 8-neighborhood. Match score between two images is calculated as the histogram intersection between their concatenated LBP histograms. This database is used for predicting matching subjects in the multiview scenario.

The results of our experiments are shown in Fig. 12. The figure shows the CMC curves of the best and worst single views: the frontal view and profile left, the results of using MM, MMR, GM and that of fusion. The rank 1, 10, 15 results are shown in Table 3. The experiments are repeated without the frontal view. The results are shown in Fig. 13 and in the tabular form in Table 4. The results show that the proposed models provide much better accuracy than the best single views and fusion (except in one case).

The non-robust multinomial model (MM) performs poorly in both experiments as underlying match scores have a significant number of outliers. However, the proposed robust approach (MMR) overcomes this limitation.

#### 4.2. Results on NIST-14 ten-print fingerprint database [31]

This database [31] consists of mated fingerprint card pairs of ten-print fingerprints from 2700 individuals. A mated fingerprint card pair means two cards from the same individual. Sample images from the database are shown in Fig. 10(a). The match score between two fingerprints is obtained by using NIST Biometric Image Software [36]. MINDTCT – a minutiae detector is used to locate and record ridge ending and bifurcations in a fingerprint image. This is fed to BOZORTH3 – a minutiae based fingerprint matching algorithm to generate the similarity scores. This database is used to carry out prediction experiments in the multiview scenario.

The results on the NIST-14 fingerprint database are shown in Fig. 14. The results are summarized in tabular form in Table 5. The GM approach gives almost 100% results on this database. Cappelli et al. [37] use the NIST-14 dataset to characterize indexing performance for subset of fingerprints and it only considers pairwise matching. While our approach gives less than 1% error for less than 1% penetration rate, Cappelli et al. [37] report error rate of approximately 9% at 1% penetration rate. This comparison provides good motivation for the use of multiple fingerprints in recognition.



Fig. 11. Sample images from the Color FERET Dataset.

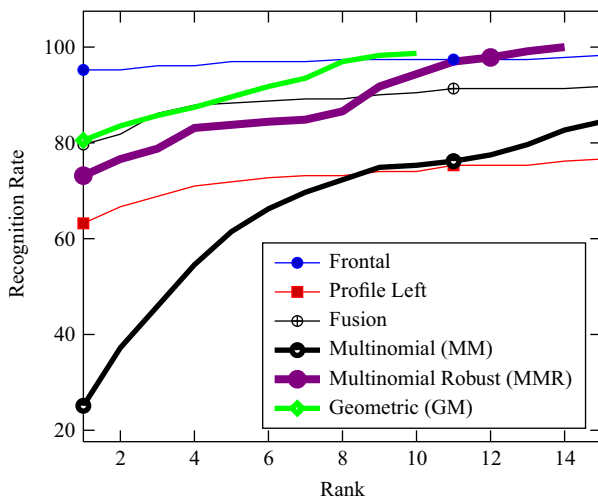


Fig. 12. CMC curves for the color FERET database. Frontal gave the best single view result and profile left gave the worst single view result. The figure shows the CMC curves of MM, multinomial model with robust estimation (MMR), and GM. Results are summarized in the tabular form in Table 3 (231 subjects).

Table 3 Rank 1, 10, 15 results on color FERET database. Bold entries show the best results and entries with underline are the second best results in each row. For a graphical representation see Fig. 12 (231 subjects).

Rank	Frontal	Profile left	Fusion	MM	MMR	GM
1	<b>95.2</b>	63.2	79.7	25.1	73.1	80.5
10	<u>97.4</u>	74.0	90.5	75.3	94.3	<b>98.7</b>
15	98.2	76.6	91.8	84.4	<b>100</b>	<u>98.7</u>

4.3. Results on the IIT Delhi iris database [32]

This database mainly consists of the iris images collected from the students and staff at IIT Delhi, New Delhi, India. This database is from 224 users and all the images are in bitmap (\*.bmp) format. Sample images from the database are shown in Fig. 10(b). The

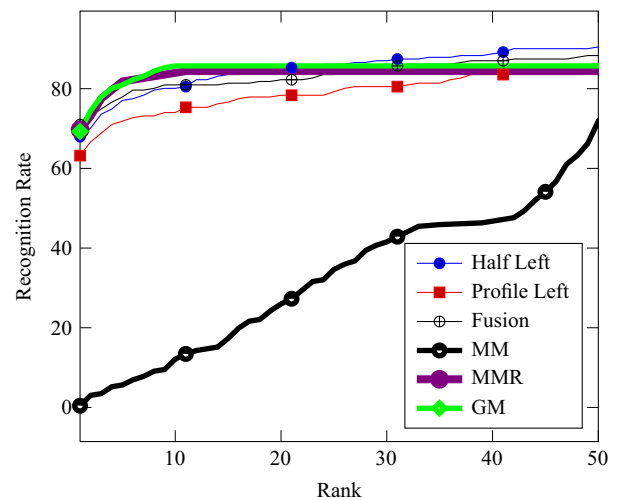


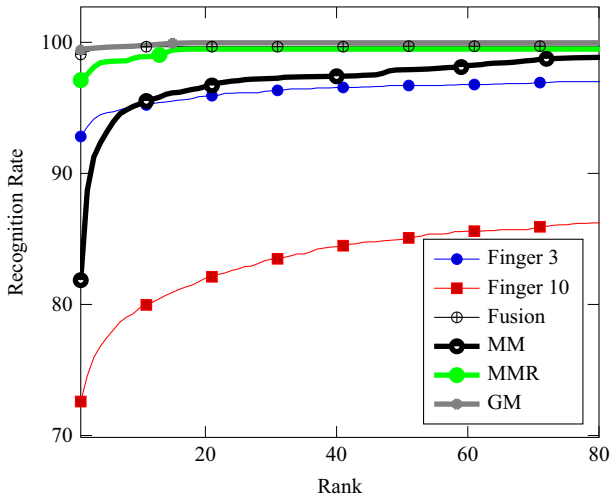
Fig. 13. CMC curves for the color FERET database without the frontal view. Half left gave the best single view result and profile left gave the worst single view result. The figure shows the CMC curves for MM, MMR, and GM and fusion. Results are summarized in the tabular form in Table 4 (231 subjects).

Table 4 Rank 1, 10, 15 results on color FERET database without the frontal view. Bold entries show the best results and entries with underline are the second best results in each row. For a graphical representation see Fig. 13 (231 subjects).

Rank	Half left	Profile left	Fusion	MM	MMR	GM
1	67.9	63.2	<b>70.9</b>	0.4	<u>69.7</u>	69.3
10	80.0	74.0	80.9	12.1	<u>83.5</u>	<b>85.7</b>
15	83.5	76.6	81.4	17.3	<u>84.4</u>	<b>85.7</b>

details of the similarity score generation are given in [38]. This database is used for multiview experiments. Two iris images are considered to be the left and right iris images of the same individual. The value of G is thus halved to 112.

The CMC curves of the proposed prediction models are shown in Fig. 15. The results are summarized in tabular form in Table 6.



**Fig. 14.** CMC curves for the NIST-14 ten-print Fingerprint Database. Finger 3 gave the best single view result and finger 10 gave the worst single view result. The plot shows the CMC curves of MM, MMR, GM and that of fusion. The prediction models outperform the individual views. For a tabular representation of the results see Table 5 (2700 subjects).

**Table 5**  
Rank 1, 10, 15 results on NIST-14 ten-print. Bold entries show the best results and entries with underline are the second best results in each row. For a graphical representation see Fig. 14 (2700 subjects).

Rank	Finger 3	Finger 10	Fusion	MM	MMR	GM
1	92.8	72.6	<u>99.0</u>	81.9	97.1	<b>99.4</b>
10	95.2	79.7	<u>99.6</u>	95.3	98.9	<b>99.7</b>
15	95.5	80.9	<u>99.7</u>	96.1	99.4	<b>99.9</b>

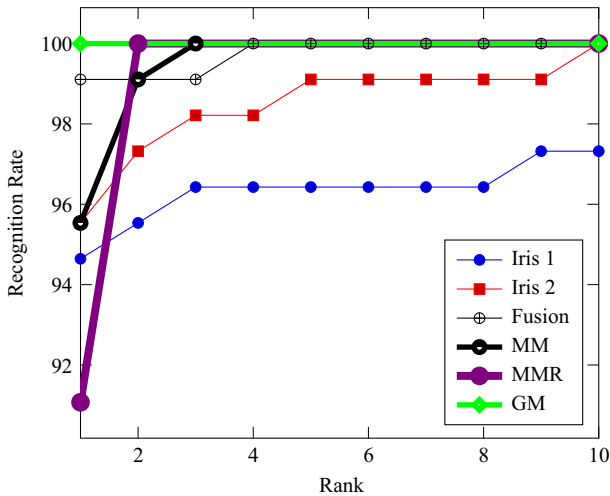


**Fig. 15.** CMC curves with IIT Delhi iris database. CMC curves for individual irises, MM, MMR, GM, and that of fusion. The results are summarized in the tabular form in Table 6 (112 subjects).

**Table 6**  
Rank 1, 10, 15 results on IIT Delhi iris database. Bold entries show the best results and entries with underline are the second best results in each row. For a graphical representation see Fig. 15. Note that MM achieves 100% success at rank 3 and MMR achieves 100% at rank 2 (112 subjects).

Rank	Iris 1	Iris 2	Fusion	MM	MMR	GM
1	94.6	95.5	<u>99.1</u>	95.5	91.0	<b>100</b>
10	97.3	99.1	100	100	100	<b>100</b>
15	97.3	100	100	100	100	<b>100</b>

**Table 7**  
Rank 1, 10, 15 results on IIT Delhi palm database. Bold entries show the best results and entries with underline are the second best results in each row. For a graphical representation see Fig. 16. Note that MM achieves 98.7% recognition rate at rank 7 and MMR achieves 97.4% success at rank 3 (116 subjects).

Rank	Palm 1	Palm 2	Fusion	MM	MMR	GM	Kumar and Shekhar [39]
1	87.1	84.5	92.2	63.8	78.4	<u>97.4</u>	<b>98.92</b>
10	93.9	91.4	98.3	<u>98.3</u>	97.4	97.4	<b>≥ 99.9</b>
15	96.6	93.1	<u>99.1</u>	98.3	97.4	97.4	<b>≥ 99.9</b>

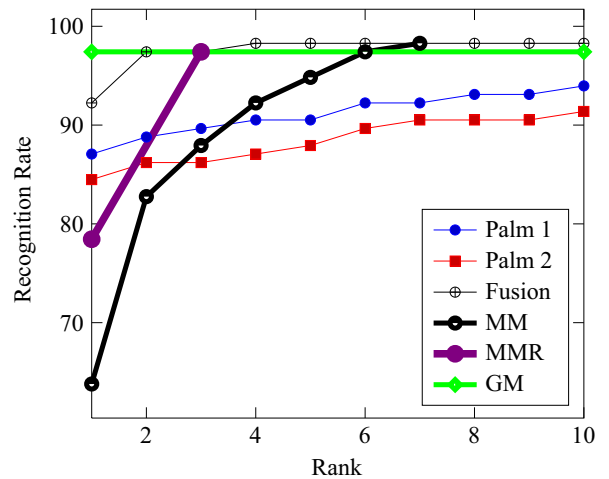


**Fig. 16.** CMC curves with IIT Delhi palm database. CMC curves for individual irises, MM, MMR, GM, and that of fusion. The results are summarized in the tabular form in Table 7 (116 subjects).

MM achieves 100% success at rank 3 and MMR achieves 100% success at rank 2. Results for IIT Delhi Iris dataset are available in the open-set identification setup in terms of a ROC curve [38] which cannot be compared with closed set identification setup used in our work.

4.4. The IIT Delhi palmprint image database [33]

This database [33] consists of the hand images collected from the students and staff at IIT Delhi, New Delhi, India. The database has images from 233 users in the bitmap (\*.bmp) format. Sample images from the database are shown in Fig. 10(c). The details of the similarity score generation are given in [39]. This database is used for multiview experiments where two palmprint images are considered to be the left and right palm images of the same individual. The value of G is thus halved to 116.

The CMC curves of the proposed models and that of individual palms are shown in Fig. 16. The results are shown in the tabular form in Table 7. The predictive models perform better than the individual views and fusion. Note that MM achieves 98.7% recognition rate at rank 7 and MMR achieves 97.4% success at rank 3.

4.5. NIST Biometric Scores Set – Release 1 (BSSR1) [34]

This is a multimodal biometrics database from the NIST [34]. It contains raw output similarity scores from face and fingerprint systems. This score set has three sets of scores. Set 1 is comprised of face and fingerprint scores from the same set of 517 individuals. For each individual, the set contains one score from the comparison of two right index fingerprints, one score from the comparison of two left index fingerprints, and two scores (from two separate matchers denoted as Face C and Face G) from the

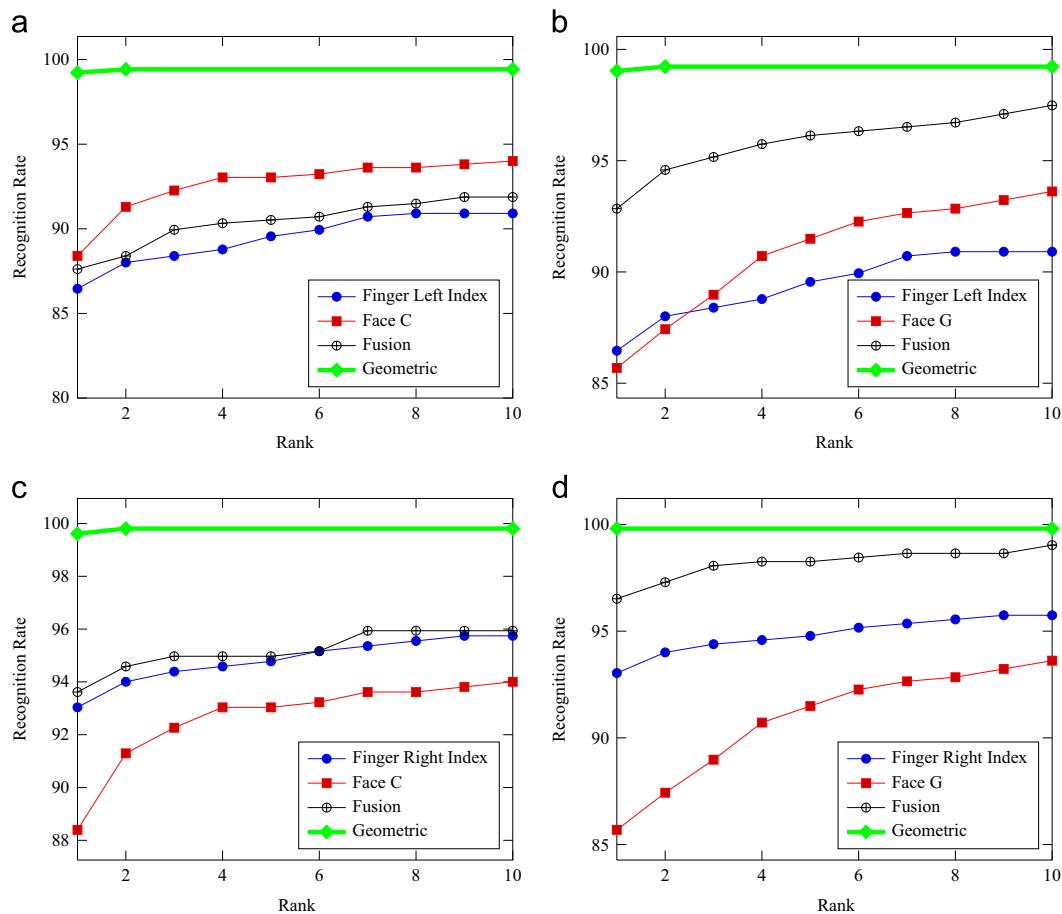


Fig. 17. NIST BSSR1 Set 1 – CMC curves of multimodal database for the four different combinations of face and fingerprint similarity scores. Note that the geometric model outperforms the fusion approach. (a) Left Index Finger and Face C, (b) Left Index Finger and Face G, (c) Right Index Finger and Face C, (d) Right Index Finger and Face G.

comparison of two frontal faces. The fingerprint images and the face images from which these scores are computed belong to the same person. The non-matching scores from the full cross-comparison are also included. As two different face and fingerprint similarity scores are available, we conduct four different multimodal experiments by combining one index finger score with one face score.

Set 2 is comprised of fingerprint scores from one system run on images of 6000 individuals. For each individual, the set contains one score from the comparison of two left index fingerprints, and another from two right index fingerprints. The non-matching scores from the left vs. left and right vs. right cross-comparisons are also included. Both of them together are used for multimodal experiments.

The results of the multimodal experiments using BSSR1 Set 1 are shown in Fig. 17. The results are shown in the tabular form in Table 8. The geometric model outperforms the fusion results and the individual view results in all the four experiments. These results may be compared with the recently published results on the same score set by Kumar et al. in [39]. They have presented two nonlinear weighted rank methods  $\exp(1)$  and  $\exp(2)$ , which combine the ranks of different matchers non-linearly. However the weight assigned to each matcher is empirically computed, the details of which are not reported. Even though the face and fingerprint scores may be combined in four different ways, it is not clear which combination of face and fingerprint scores is used in that work. In contrast, the proposed method does not use any empirical constants and the results on all the four combinations are shown in Fig. 17 and Table 8. The average recognition rates of

Table 8

Rank 1,2,3 results on NIST BSSR1 – Set 1, Fingerprint and Face database (517 subjects).

Modalities	Rank	Finger	Face	Fusion	GM
Left Index Finger and Face C	1	86.5	88.4	87.6	<b>99.2</b>
	2	88.0	91.3	88.3	<b>99.4</b>
	3	88.4	92.3	89.9	<b>99.4</b>
Left Index Finger and Face G	1	86.5	85.7	92.8	<b>99.0</b>
	2	88.0	87.4	94.6	<b>99.2</b>
	3	88.4	88.9	95.2	<b>99.2</b>
Right Index Finger and Face C	1	93.0	88.4	93.6	<b>99.6</b>
	2	94.0	91.3	94.6	<b>99.8</b>
	3	94.4	92.3	94.9	<b>99.8</b>
Right Index Finger and Face G	1	93.0	85.7	96.5	<b>99.8</b>
	2	94.0	87.4	97.3	<b>99.8</b>
	3	94.4	88.9	98.1	<b>99.8</b>

the two methods reported in [39] are 99.56%, 99.59%, and 100% for Rank 1, 2, 3 recognition, respectively. The method proposed in this paper outperforms these results (Rank 1 recognition rate of 99.8% for right index finger and face G combination).

Using BSSR1 set 2 database one more multimodal experiment was conducted. The results are shown in Fig. 18. The results are shown in the tabular form in Table 9. The results are compared with fusion and those published recently in [39]. The results obtained using the GM are better than those reported in [39] and better than fusion for rank 2 and rank 3 but not for rank 1.

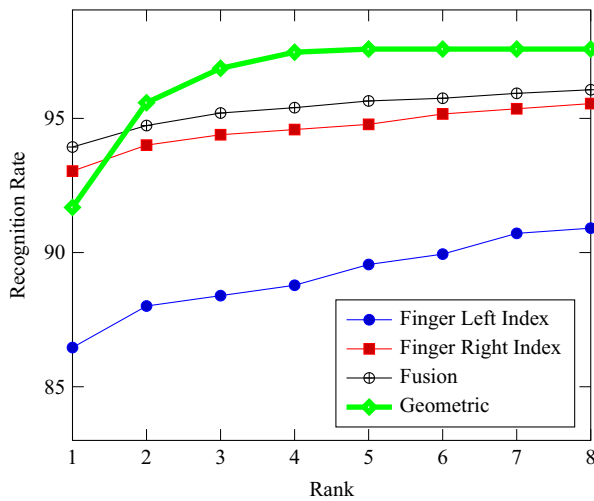


**Fig. 18.** CMC curves obtained by combining Left and Right index finger scores of BSSR1 Set 2 scoreset (6000 subjects).

**Table 9**

Rank 1, 2, 3 results on NIST BSSR1 - Set 2 database containing right and left index finger scores (6000 subjects).

Rank	LI	RI	Fusion	GM	Kumar and Shekhar [39]
1	86.5	93.0	<b>93.9</b>	91.7	89.5
2	88.0	94.0	<u>94.7</u>	<b>95.6</b>	94.2
3	88.4	94.4	95.2	<b>97.5</b>	<u>95.2</u>

#### 4.6. Discussion of experimental results

The geometric model performs better in our experiments for two reasons. First, the view information is available. This is an extra knowledge for GM which is not available for MM. Second, as there are  $V$  different databases, each test subject corresponding to specific view or modality is matched against only  $G$  database subjects in contrast to  $GV$  subjects in the MM case. Clearly, in cases where view details are available and/or modalities of biometrics are different, the geometric model should be preferred over the multinomial model. On the other hand, the multinomial model can be used in more unconstrained environment where view details of the object are unknown.

## 5. Conclusions

Two novel statistical models which can lead to the prediction of the matching subjects for multibiometric systems are presented. It is shown through a variety of experiments that the prediction framework enhances the recognition rate of the underlying matching algorithm. Ten different experiments are conducted with five different publicly available databases. Results of these experiments show that using the proposed generic predictive models, the recognition can be improved for variety of multibiometrics such as multiple face views, fingerprints, palm prints and irises using the same modeling framework.

#### Conflict of interest

None declared.

## References

- [1] K. Ricanek, Dissecting the human identity, *IEEE Comput.* 44 (January (1)) (2011) 96–97.
- [2] A. Ross, A.K. Jain, Multimodal biometrics: an overview, in: *Proceedings of the 12th European Signal Processing Conference (EUSIPCO)*, Vienna, Austria, September 2004, pp. 1221–1224.
- [3] B. Bhanu, V. Govindaraju (Eds.), *Multibiometrics for Human Identification*, Cambridge University Press, New York, 2011.
- [4] K. Bowyer, K. Chang, P. Flynn, X. Chen, Face recognition using 2-D, 3-D, and infrared: is multimodal better than multisample? *Proc. IEEE* 94 (November (11)) (2006) 2000–2012.
- [5] K. Chang, K. Bowyer, P. Flynn, An evaluation of multimodal 2D+3D face biometrics, *IEEE Trans. Pattern Anal. Mach. Intell.* 27 (April (4)) (2005) 619–624.
- [6] DHS, Biometrics Standards Requirements for US-Visit. URL ([http://www.dhs.gov/xlibrary/assets/usvisit/usvisit\\_biometric\\_standards.pdf](http://www.dhs.gov/xlibrary/assets/usvisit/usvisit_biometric_standards.pdf)).
- [7] D. Gorodnichy, Evolution and evaluation of biometric systems, in: *IEEE Symposium on Computational Intelligence for Security and Defense Applications*, July 2009, pp. 1–8.
- [8] J.L. Wayman, Error rate equations for the general biometric system, *IEEE Robot. Autom. Mag.* 6 (August (1)) (2002) 35–48.
- [9] J. Daugman, The importance of being random: statistical principles of iris recognition, *Pattern Recognit.* 36 (2) (2003) 279–291.
- [10] P.J. Phillips, P. Grother, R.J. Micheals, D.M. Blackburn, E. Tabassi, M. Bone, *Face Recognition Vendor Test 2002: Evaluation Report*, 2003.
- [11] A.Y. Johnson, J. Sun, A.F. Bobick, Using similarity scores from a small gallery to estimate recognition performance for larger galleries, *IEEE International Workshop on Analysis and Modeling of Faces and Gestures*, 2003, p. 100.
- [12] R. Wang, B. Bhanu, Predicting fingerprint biometrics performance from a small gallery, *Pattern Recognit. Lett.* 28 (January) (2007) 40–48.
- [13] P. Grother, P. Phillips, Models of large population recognition performance, in: *CVPR 2004*, vol. 2, June 2004, pp. II-68–II-75.
- [14] S.C. Dass, Y. Zhu, A.K. Jain, Validating a biometric authentication system: sample size requirements, *IEEE Trans. Pattern Anal. Mach. Intell.* 28 (2006) 1902–1919.
- [15] P. Wang, Q. Ji, J. Wayman, Modeling and predicting face recognition system performance based on analysis of similarity scores, *IEEE Trans. Pattern Anal. Mach. Intell.* 29 (April (4)) (2007) 665–670.
- [16] N. Schmid, J. O'Sullivan, Performance prediction methodology for biometric systems using a large deviations approach, *IEEE Trans. Signal Process.* 52 (October (10)) (2004) 3036–3045.
- [17] M. Boshra, B. Bhanu, Predicting performance of object recognition, *IEEE Trans. Pattern Anal. Mach. Intell.* 22 (2000) 956–969.
- [18] G. Aggarwal, S. Biswas, P. Flynn, K. Bowyer, Predicting performance of face recognition systems: an image characterization approach, in: *CVPRW2011*, June 2011, pp. 52–59.
- [19] S. Pankanti, S. Prabhakar, A. Jain, On the individuality of fingerprints, *IEEE Trans. Pattern Anal. Mach. Intell.* 24 (August (8)) (2002) 1010–1025.
- [20] X. Tan, B. Bhanu, On the fundamental performance for fingerprint matching, in: *IEEE Computer Society Conference on Computer Vision and Pattern Recognition*, vol. 2, June 2003, pp. II-499–II-504.
- [21] S. Kumar, B. Bhanu, S. Ghosh, N. Thakoor, Prediction and validation of indexing performance for biometrics, in: *International Joint Conference on Biometrics*, 2011.
- [22] A.M. Mood, *Introduction to the Theory of Statistics*, McGraw Hill Book Company Inc., 1950, p. 55.
- [23] NIST, NIST Color Feret DataSet. URL (<http://www.nist.gov/humanid/colorferet>).
- [24] V. Rohatgi, *An Introduction to Probability Theory and Mathematical Statistics*, John Wiley, New York, 1976.
- [25] H. Kast, A. Kim, A. Paisoseputra, S.V. Kirk, *Michigan Chemical Engineering Process Dynamics and Controls Open Textbook*, University of Michigan, 2007. URL ([http://controls.engin.umich.edu/wiki/index.php/Main\\_Page](http://controls.engin.umich.edu/wiki/index.php/Main_Page)).
- [26] K. Nigam, A.K. McCallum, S. Thrun, T. Mitchell, Text classification from labeled and unlabeled documents using EM, *Mach. Learn.* 39 (May (2–3)) (2000) 103–134.
- [27] A. Agresti, *An Introduction to Categorical Data Analysis*, Wiley, New York, 1996.
- [28] R.D.M. Ricardo, A. Maronna, V.J. Yohai, *Robust Statistics Theory and Methods*, John Wiley & Sons Ltd., Chichester, West Sussex, England, 2006.
- [29] K. Konis, Package Robust. URL (<http://cran.r-project.org/web/packages/robust/robust.pdf>), April 2012.
- [30] A. Papoulis, S.U. Pillai, *Probability, Random Variables and Stochastic Processes*, McGraw Hill, New York, 2002.
- [31] NIST, NIST Special Database 14. URL (<http://www.nist.gov/srd/nistsd14.cfm>).
- [32] Indian Institute of Technology Delhi, IIT Delhi Iris Database (Version 1.0). URL ([http://www4.comp.polyu.edu.hk/~csajaykr/IITD/Database\\_Iris.htm](http://www4.comp.polyu.edu.hk/~csajaykr/IITD/Database_Iris.htm)).
- [33] I.I.T. Delhi, Touchless Palmprint Database (Version 1.0). URL ([http://www4.comp.polyu.edu.hk/~csajaykr/IITD/Database\\_Palm.htm](http://www4.comp.polyu.edu.hk/~csajaykr/IITD/Database_Palm.htm)).
- [34] NIST, NIST Biometric Score Set. URL (<http://www.itl.nist.gov/iad/894.03/biometricscores/>).
- [35] S. Yang, B. Bhanu, Understanding discrete facial expressions in video using an emotion avatar image, *IEEE Trans. Syst. Man Cybern. B* 42 (August (4)) (2012) 980–992.

- [36] NIST, NIST Biometric Image Software. URL (<http://www.nist.gov/itl/iad/ig/nbis.cfm>).
- [37] R. Cappelli, M. Ferrara, D. Maltoni, Fingerprint indexing based on minutia cylinder-code, *IEEE Trans. Pattern Anal. Mach. Intell.* 33 (May (5)) (2011) 1051–1057.
- [38] A. Kumar, A. Passi, Comparison and combination of iris matchers for reliable personal authentication, *Pattern Recognit.* 43 (3) (2010) 1016–1026.
- [39] A. Kumar, S. Shekhar, Personal identification using multibiometrics rank-level fusion, *IEEE Trans. Syst. Man Cybern. C* 41 (September (5)) (2011) 743–752.

**Suresh Kumar Ramachandran Nair** received his bachelor's degree from the College of Engineering, Trivandrum, India. He completed master's degree in system science and automation from the Indian Institute of Science, Bangalore, India in 1997. He started pursuing PhD in electrical engineering from 2009. His research interests include performance prediction, statistical modeling, biometrics, pattern recognition and machine learning.

**Bir Bhanu** is the Distinguished Professor of Electrical Engineering and a Cooperative Professor of Computer Science and Engineering, Bioengineering, and Mechanical Engineering, and Director of the Center for Research in Intelligent Systems (CRIS), and the Visualization and Intelligent Systems Laboratory (VISLab) at the University of California, Riverside (UCR). Dr. Bhanu received the S.M. and E.E. degrees in Electrical Engineering and Computer Science from the Massachusetts Institute of Technology; the Ph.D. degree in Electrical Engineering from the Image Processing Institute, University of Southern California and the M.B.A. degree from the University of California, Irvine. Dr. Bhanu's current research interests are Computer Vision, Pattern Recognition and Data Mining, Machine Learning, Artificial Intelligence, Image, Image and Video Database, Graphics and Visualization, Robotics, Human–Computer Interactions, Biological, Medical, Military and Intelligence applications.

**Subir Ghosh** is a Professor in Department of Statistics at University of California Riverside. He received M.S. in Statistics from University of Calcutta, India in 1970 and Ph.D. in Statistics from Colorado State University, Fort Collins, USA in 1976. He is an elected fellow of American Statistical Association and American Association for the Advancement of Science. His research interests are in statistical design and analysis of experiments, linear models, industrial statistics, sample surveys, longitudinal data analysis, econometrics, and social statistics.

**Ninad Thakoor** received the BE degree in electronics and telecommunication engineering from the University of Mumbai, India, in 2001, and the MS and PhD degrees in electrical engineering from the University of Texas at Arlington, in 2004 and 2009, respectively. His research interests include object recognition, stereo disparity segmentation, and structure-and-motion segmentation. Currently he is with the Center for Research in Intelligent Systems at the University of California at Riverside.